ChemComm

ROYAL SOCIETY OF CHEMISTRY

COMMUNICATION

View Article Online
View Journal | View Issue

Cite this: *Chem. Commun.*, 2025, **61**, 2111

Received 14th September 2024,
Accepted 22nd December 2024

DOI: 10.1039/d4cc04765f

rsc.li/chemcomm

Microwave assisted synthesis of Ti_3C_2-MXene for supercapacitor application†

Prasad Eknath Lokhande, *[a] Udayabhaskar Rednam,*[a] Vishal Kadam,[b] Chaitali Jagtap,[b] Deepak Kumar [c] and Radhamanohar Aepuru[d]

Two-dimensional Ti_3C_2 MXene has been successfully synthesized using an ultrafast microwave-assisted method. Material characterization studies have confirmed the formation of a layered MXene structure. Additionally, the electrochemical performance observed for the synthesized material indicates its promising potential for use in supercapacitor applications.

Since the discovery of the two-dimensional (2D) Ti_3C_2-MXene in 2011, the MXene family has been expanding, and its applications have been growing due to outstanding properties such as excellent electrical conductivity, high surface area, and hydrophilic nature.[1] MXenes are synthesized from the MAX phase ($M_{n+1}AX_n$), where M represents transition metals, A stands for main group elements, and X is carbon and/or nitrogen. The process involves selectively etching the A layer from the MAX phase to produce MXene ($M_{n+1}X_nT_x$).[1] Traditionally, this is achieved using hydrofluoric (HF) acid, which can take hours for complete etching. Over time, alternative synthesis methods have been developed,[2–4] including selective etching with LiF + HCl, alkali (NaOH), and molten salt, yet these methods also require hours to complete the synthesis.

The characteristics of MXene have garnered significant interest in the field of energy storage such as in supercapacitors. Kumar *et al.* synthesized nano-layered MXene as an active electrode material, $Ti_3C_2T_x$, from the supernatant during a 48-hour etching process, which demonstrated a high specific capacitance of approximately 542 F g^{-1} at a 5 mV s^{-1} scan rate, according to cyclic voltammetry analysis.[5] Wu *et al.* synthesized a few layers of Ti_3C_2 using an etching and subsequent microwave-assisted hydrothermal technique, where the layers became more distorted under the combined action of the etching agent and microwave hydrothermal solution, eventually fracturing and dissociating. The resulting material exhibited a specific capacitance of 418.07 F g^{-1}.[6] The same research group further synthesized free-standing Ti_3C_2 using a Lewis acid molten salt method and microwave-assisted etching method, which showed a specific capacitance of 347.24 F g^{-1} at 1 A g^{-1} with superior cyclic stability.[7] Both of these synthesis processes took hours. Since these synthesis methods are time-consuming, it is of paramount importance to develop a new method that can synthesize MXene more quickly. Additionally, the quality of the synthesized MXene must be maintained from an energy storage perspective.

This study marks the first instance of synthesizing Ti_3C_2 MXene in a single step, achieved in mere seconds through a microwave-assisted method tailored for supercapacitor applications. The process utilizes HF etching to remove Al from the MAX phase, expedited by microwave energy. Structural and morphological analyses have verified the formation of undistorted, layered MXene. Electrochemical evaluations of the synthesized material revealed outstanding performance metrics. Additionally, the constructed asymmetric supercapacitor device showcased exceptional energy and power densities, coupled with remarkable cyclic stability.

Starting with 1 g of Ti_3AlC_2 MAX phase in a Teflon-coated ceramic crucible, 10 mL of 48% hydrofluoric acid (HF) was added. The mixture was then exposed to microwave irradiation at 600 W and 2.5 GHz for 30 seconds. After microwave treatment, the product was repeatedly washed with deionized water until reaching a neutral pH of 5. Finally, the washed material was incubated at 70 °C for 12 hours, resulting in the dry MXene powder. Synthesized material was characterized for the confirmation of formation of MXene and etching of Al layer. Further synthesized material was used for supercapacitor application.

The $Ti_3C_2T_x$ was synthesized from the Ti_3AlC_2 MAX phase using a rapid microwave-assisted method, where HF served as the etching agent. The HF treatment aimed to etch the

[a] *Departamento de Mecanica, Facultad de Ingenieria, Universidad Tecnologica Metropolitana, Santiago, Chile. E-mail: p.eknath@utem.cl, uday.rednam@utem.cl*
[b] *Advanced Physics Laboratory, Department of Physics, Savitribai Phule Pune University, Pune, India*
[c] *Department of Chemistry, School of Chemical Engineering and Physical Sciences, Lovely Professional University, Phagwara – 144411, India*
[d] *Departamento de Ingeniería Mecánica, Facultad de Ciencias Fisicas y Matematicas, Universidad de Chile, Beauchef, 8370456, Santiago, Chile*

† Electronic supplementary information (ESI) available. See DOI: https://doi.org/10.1039/d4cc04765f

aluminum from the MAX phase to form $Ti_3C_2T_x$ with some functional groups attached to the surface. The possible reactions that occurred during this process are as follows:[8]

$$Ti_3AlC_2 + 3HF \rightarrow AlF_3 + \frac{3}{2}H_2 + Ti_3C_2 \quad (1)$$

$$Ti_3C_2 + 2H_2O \rightarrow Ti_3C_2(OH)_2 + H_2 \quad (2)$$

$$Ti_3C_2 + 2HF \rightarrow Ti_3C_2F_2 + H_2 \quad (3)$$

Reaction (1) was succeeded by reactions (2) and (3). In the current synthesis method, microwave energy aids in etching aluminum at an accelerated rate, and the residual dry powder suggests that the predominant functional group attached to the surface will be fluorine (F).

The microwave-assisted synthesis of MXene was characterized to obtain crystallographic and morphological information. The XRD peaks for Ti_3AlC_2-MAX phase and $Ti_3C_2T_x$ MXene, as shown in Fig. 1(a), include a peak at 8.7°, attributed to the (002) plane, which is typically found at 9.7° for the Ti_3AlC_2 MAX phase. The shift of this peak towards a lower angle confirms the formation of $Ti_3C_2T_x$. Additionally, the peak intensity of 39°, corresponding to the (104) plane, is characteristic of the Ti_3AlC_2 MAX phase. In the current XRD graph for $Ti_3C_2T_x$, the reduced intensity indicates that the etching of Al has occurred during the synthesis process. The FTIR spectra obtained spectra for Ti_3AlC_2-MAX phase and $Ti_3C_2T_x$ shown in Fig. 1(b). The absorption peaks at 1639 cm^{-1} and 3549 cm^{-1} are ascribed to the presence of absorbed external water and a strongly hydrogen-bonded OH group, respectively. The microwave synthesis yielded a dry powder, implying a diminished presence of the OH group, as evidenced by the weak absorption at 3449 cm^{-1}. The peak at 571 cm^{-1} is indicative of the O–Ti–O lattice stretching vibration found in TiO_2, and the peak at 645 cm^{-1} is associated with the Ti–O deformation vibration. Additionally, the peaks at 1530, 2302, and 2921 cm^{-1} are representative of the –C═C–, CO_2, and $–CH_2$ functional groups, respectively. The pronounced peaks at 1901 and 2101 cm^{-1}, typically not reported in the literature, are indicative of the asymmetric stretching of the C═O bond. The study indicated the presence of –F functional groups in minimal quantities, suggesting the formation of $Ti_3C_2T_x$ MXene with surface functional groups.

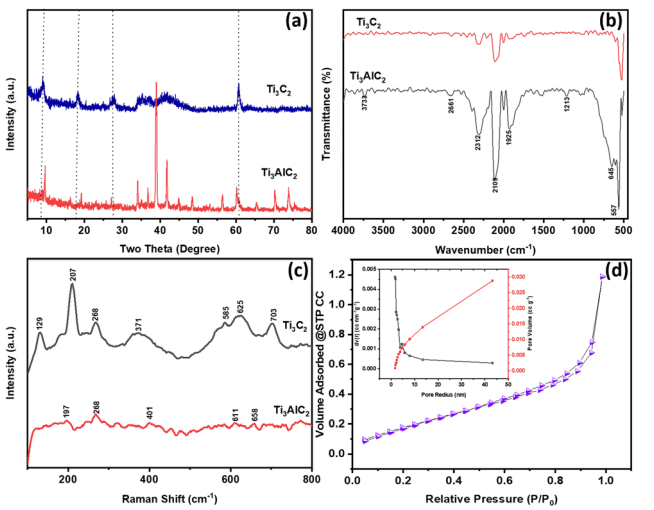

Fig. 1 (a) XRD peak obtained for Ti_3AlC_2-MAX phase and $Ti_3C_2T_x$ (b) FTIR spectra (c) Raman peak obtained for MAX phase MXene (b) nitrogen adsorption and desorption isotherms of the $Ti_3C_2T_x$.

The study of chemical bonding and intramolecular bonds was advanced through Raman spectroscopy, with the resulting spectra displayed in Fig. 1(c). Typically, spectral regions are crucial in the Raman analysis of MXene: the low-frequency range (100–800 cm^{-1}), which is attributed to lattice vibrations, and the high-frequency range (1000–1800 cm^{-1}), which corresponds to the C–C stretching vibrations in the carbon structure of MXene. It has been noted that the terminal atoms significantly affect the vibrational mode frequencies. In this study, the primary peaks at 129, 207, 371, 585, and 625 cm^{-1} are indicative of the formation of $Ti_3C_2T_x$ with functional groups such as –OH and –F. The pronounced intensity of these peaks may be due to increased laser power, which could lead to the oxidation of $Ti_3C_2T_x$. The TiO_2 that forms from MXene can exist in two crystalline forms: rutile and anatase, with the anatase phase appearing first and requiring less energy to form. This anatase phase is identified by the most intense band at 129 cm^{-1}, associated with the E_g mode, and the study's intense peak at 129 cm^{-1} confirms the formation of the anatase phase.[9] This is further corroborated by the spectral band at 625 cm^{-1}, also associated with the E_g mode. Additionally, the spectrum at 207 cm^{-1} is related to the out-of-plane vibrations of the Ti and carbon atoms. The surface area and pore size distribution of the sample were assessed using the BET and BJH methods, as well as the nitrogen adsorption–desorption curve depicted in Fig. 1(d). The surface area of the sample measured 12.99 $m^2\ g^{-1}$, and the average pore size was determined to be 1.68 nm. The surface morphological features of the synthesized material were examined using field emission scanning electron microscopy (FESEM), and the images are shown in Fig. 2. Fig. 2(a)–(c) provide a side view of the layered $Ti_3C_2T_x$, revealing well-separated layers after microwave-assisted HF treatment, as opposed to the densely packed structure of Ti_3AlC_2. The interlayer spacing in the $Ti_3C_2T_x$ was measured at 0.30 μm, significantly greater than that found in the MAX phase. These results indicate the successful removal of aluminium layers from the MAX phase. The FESEM images reveal intact layers without the distortions typically reported in previous literature, which are attributed to microwave treatment.[6,10] Furthermore, no additional small particles, such as AlF_3, which have been observed in other studies, were detected. EDS spectra obtained for $Ti_3C_2T_x$ shown in Fig. 2(d) which demonstrates the lower percentage of Al. Further XPS analysis was carried out and obtained results shown in Fig. S1 (ESI†) which are agreement with XRD. In present study, TiO_2 typically forms due to oxidation, implying that exposure of $Ti_3C_2T_x$ to oxygen can cause some titanium atoms within its structure to oxidize, resulting in the formation of TiO_2 on the surface of the MXene sheets which also confirm from XPS results.[11–13]

The electrochemical assessments were conducted on a three-electrode setup within an electrochemical workstation,

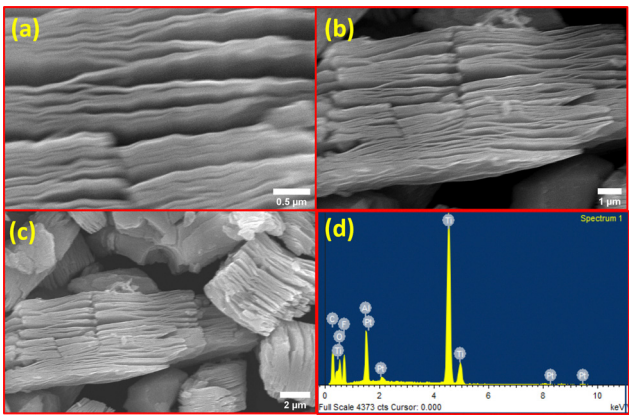

Fig. 2 (a)–(c) FESEM images at various magnification (d) EDS spectra of $Ti_3C_2T_x$.

employing a 1 M H_2SO_4 electrolyte solution. The CV curves for $Ti_3C_2T_x$, depicted in Fig. 3(a), were recorded at varying scan rates of 10, 20, 30, 40, 50, and 100 mV s^{-1}, utilizing an optimized potential window ranging from −0.2 to 0.4 V. These curves exhibited distinct pseudocapacitive behaviour. The maximum specific capacitance values for the prepared sample were determined to be 96 F g^{-1} at corresponding scan rates of 10 mV s^{-1}. This enhancement in specific capacitance can be attributed to the facile diffusion of the electrolyte ions, a reduced diffusion path, and an interlayer spacing that is conducive to ion diffusion.

To further confirm the electrochemical performance, the GCD technique was employed, and the resulting GCD profile is depicted in Fig. 3(b) at various current densities. The symmetric and non-linear profile corroborates the pseudocapacitive behaviour, aligning with the CV results. Specific capacitances of 245, 208, 139, 86, 45, and 35 F g^{-1} were recorded at current densities of 5, 10, 15, 20, 25, and 30 A g^{-1}, respectively. The –O functional

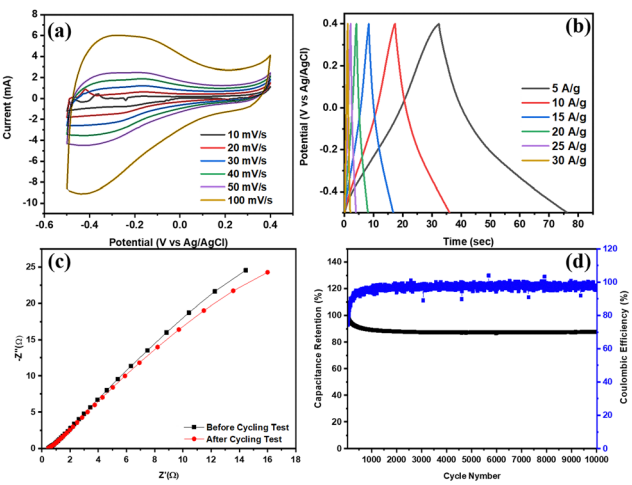

Fig. 3 (a) CV curve at scan rate of 10, 20, 30, 40, 50 and 100 mV s^{-1}. (b) GCD profile at current density of 5, 10, 15, 20, 25, and 30 A g^{-1}. (c) Nyquist plot before and after cycling stability test. (d) Cyclic stability and coulombic efficiency tested for $Ti_3C_2T_x$ electrode for 10 000 cycles.

groups on the $Ti_3C_2T_x$ surface contribute to the enhanced electrochemical performance.[14] The rapid synthesis method for MXene causes the HF etchant to evaporate, and small amount of –F group remain even after washing. The electrochemical performance improvement is attributed to this additional interlayer space and functional groups. The electrochemical resistance study is crucial as it determines the variation in ion transport resistance and the impact of increased conductivity on reducing internal resistance. The Nyquist plot from the EIS study, shown in Fig. 3(c), along with the equivalent circuit used for fitting, indicates that the plot's intersection with the *X*-axis provides the R_s or internal resistance value. This was found to be 0.68 Ω, significantly lower than the literature values for $Ti_3C_2T_x$, likely due to the improved conductive network in the prepared material. The diameter of the semicircle in the Nyquist plot represents the R_{ct} or charge transfer resistance, which was found to be 1.23 Ω, again lower than the literature values. This reduced charge transfer resistance could be attributed to an increased interplanar distance, facilitating ion diffusion. The cyclic stability study is a crucial analysis in the field of energy storage, assessing the material's ability to maintain electrochemical performance over numerous cycles. The cyclic stability test, conducted on the microwave-assisted $Ti_3C_2T_x$ for 10 000 cycles as depicted in Fig. 3(d), revealed 88% retention of capacitance after the completion of the cycles. These results indicate the synthesized MXene's potential for long-term durability.

The feasibility of the prepared material in practical applications was evaluated by fabricating an asymmetric solid-state supercapacitor device. The prepared material, $Ti_3C_2T_x$ was used as the positive electrode, and activated carbon (AC) was used as the negative electrode, with PVA/KOH gel as the electrolyte. The CV curve for the fabricated device $Ti_3C_2T_x$/Ni//AC/Ni, shown in Fig. 4(a), was tested at scan rates of 1, 5, 10, 20, 30, 40, 50, and 100 mV s^{-1}. The exhibited CV curve demonstrates hybrid behaviour, showing pseudocapacitance from $Ti_3C_2T_x$ and EDLC-type behaviour from activated carbon. Further, the GCD technique was used to evaluate the electrochemical performance of the fabricated device, and the obtained GCD profile is shown in Fig. 4(b) at current densities of 1, 2, 3, and 4 A g^{-1}. The device exhibited a maximum specific capacitance of 75 F g^{-1} at a current density of 1 A g^{-1}. The energy density and power density of the device were measured to be 23 W h kg^{-1} and 750 W kg^{-1}, respectively. An electrochemical resistance study was conducted on the fabricated device using the EIS technique, which yielded the Nyquist plot depicted in Fig. 4(c). The gel electrolyte resistance (R_1) measured for the device was 2.67 Ω, and the charge transfer resistance (R_2) was 3.98 Ω. The use of a gel electrolyte in the current device fabrication resulted in a slightly higher resistance. Another important parameter, cyclic stability, was evaluated by testing the supercapacitor device for 10 000 cycles, as shown in Fig. 4(d), with a capacitance retention of more than 100% after 10 000 cycles. Performance improved with an increasing number of cycles due to nickel foam is used as the substrate material. After several cycles, the intrinsic materials in the nickel foam provide additional active sites, which further enhancing performance. The results for the electrode and fabricated device indicate the potential of $Ti_3C_2T_x$ in supercapacitor applications. Furthermore, the current method enables the synthesis of MXene in

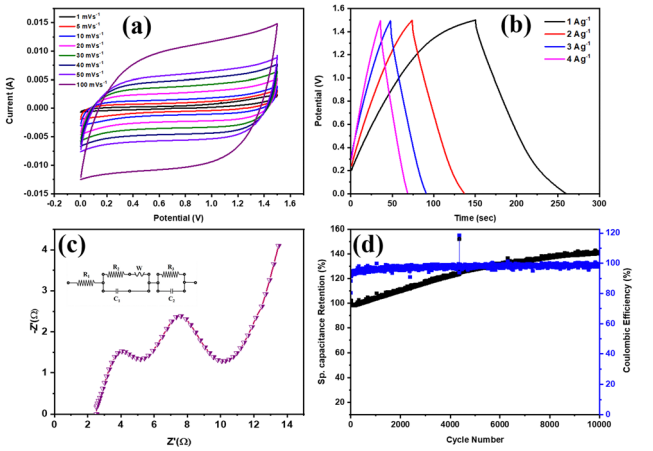

Fig. 4 (a) CV curve at various scan rates of (b) GCD profile at various current densities (c) Nyquist plot (inside: equivalent circuit) (d) cyclic stability and coulombic efficiency at 10 000 cycles for $Ti_3C_2T_x$//AC all solid-state supercapacitor device.

substantial quantities within a brief period, which is beneficial for various applications. However, an increase in synthesis time may lead to more defects.

In summary, $Ti_3C_2T_x$ MXene was rapidly synthesized *via* a microwave-assisted method, bypassing traditional HF etching. Characterization revealed Al-etched MXene with a larger interplanar distance and a layered structure. Electrochemically, $Ti_3C_2T_x$ exhibited a high specific capacitance of 282 F g^{-1} at 5 A g^{-1} and reduced charge transfer resistance. A device made from this MXene showed an energy density of 23 W h kg^{-1}, a power density of 750 W kg^{-1}, and outstanding cyclic stability. These results indicate that $Ti_3C_2T_x$ MXene is a promising material for energy storage solutions.

P. E. Lokhande: writing original draft, data curation, editing draft, methodology, conceptualization, funding acquisition; Udayabhaskar Rednam: formal analysis, supervision, investigation; Chaitali Jagtap: investigation; Vishal Kadam: data curation, formal analysis; Deepak Kemar: data curation, formal analysis; Radhamanohar Aepuru: data curation, formal analysis.

The author P. E. L. acknowledges ANID for the financial support through project FONDECYT#3230388. The author R. U. acknowledges ANID, Chile for the financial support through project FONDECYT# 11220335. The R. U. acknowledges "FESEM-Proyecto UTM1999" and "Project supported by the Fund for Scientific and Technological Equipment, year 2023, code LE23-01, Universidad Tecnológica Metropolitana". UTEM, Santiago, CHILE for BET characterization studies support.

Data availability

All data obtained during the experimentation is reported in the manuscript and ESI.†

Conflicts of interest

There are no conflicts to declare.

Notes and references

1 P. E. Lokhande, A. Pakdel, H. M. Pathan, D. Kumar, D.-V. N. Vo, A. Al-Gheethi, A. Sharma, S. Goel, P. P. Singh and B.-K. Lee, *Chemosphere*, 2022, **297**, 134225.
2 X. Shi, Z. Yu, Z. Liu, N. Cao, L. Zhu, Y. Liu, K. Zhao, T. Shi, L. Yin and Z. Fan, *Angew. Chem., Int. Ed.*, 2024, e202418420.
3 Y. Wang, B. Zhou, Q. Tang, Y. Yang, B. Pu, J. Bai, J. Xu, Q. Feng, Y. Liu and W. Yang, *Adv. Mater.*, 2024, 2410736.
4 L. Sun, J. Xie, L. Zhang, R. Jiang, J. Wu, L. Fan, R. Shao, Z. Chen and Z. Jin, *FlatChem*, 2020, **20**, 100152.
5 S. Kumar, M. A. Rehman, S. Lee, M. Kim, H. Hong, J.-Y. Park and Y. Seo, *Sci. Rep.*, 2021, **11**, 649.
6 Q. Wu, Y. Wang, P. Li, S. Chen and F. Wu, *J. Electrochem. Soc.*, 2021, **168**, 090549.
7 Q. Wu, P. Li, Y. Wang and F. Wu, *Appl. Surf. Sci.*, 2022, **593**, 153380.
8 M. Naguib, M. Kurtoglu, V. Presser, J. Lu, J. Niu, M. Heon, L. Hultman, Y. Gogotsi and M. W. Barsoum, *Adv. Mater.*, 2011, **23**, 4248–4253.
9 S. Adomaviciute-Grabusove, A. Popov, S. Ramanavicius, V. Sablinskas, K. Shevchuk, O. Gogotsi, I. Baginskiy, Y. Gogotsi and A. Ramanavicius, *ACS Nano*, 2024, **18**, 13184–13195.
10 X. Wang, N. Han, Y. Zhang, G. Shi, Y. Zhang and D. Li, *J. Mater. Sci.: Mater. Electron.*, 2022, **33**, 21091–21100.
11 C. Lai, B. Yan, R. Yuan, D. Chen, X. Wang, M. Wang, H. He and J. Tu, *RSC Adv.*, 2023, **13**, 16222–16229.
12 D. B. Salunkhe, S. S. Gargote, D. P. Dubal, W. B. Kim and B. R. Sankapal, *Chem. Phys. Lett.*, 2012, **554**, 150–154.
13 B. R. Sankapal, S. D. Sartale, M. C. Lux-Steiner and A. Ennaoui, *C. R. Chim*, 2005, **9**, 702–707.
14 L. Liu, E. Raymundo-Piñero, S. Sunny, P. Taberna and P. Simon, *Angew. Chem., Int. Ed.*, 2024, **63**, e202319238.

